Development of the Shim-Joint Concept for Composite Structural Members

J. P. Wong,* B. W. Cole,† and A. L. Courtney‡
The Bendix Corporation, South Bend, Ind.

This paper describes a shim-joint concept that was developed to improve the efficiency of joints for attaching to composite material structural members. The shim-joint concept reinforces the composite material in the region of the joint with thin metallic layers which permits employing a conventional shear pin joint between the composite members and a mating fitting. Design parameters are defined and design data are established. Improved methods for fabricating the reinforced tube ends and improved testing fixtures are developed. An advanced optimization technique has been applied to the design of the shim joints. It is shown that design parameters can be optimized conveniently by the structural synthesis approach in determining the minimum weight configuration. The results indicate that the shim-joint concept can be successfully applied to composite members without prohibitive attachment weight penalties.

Nomenclature

a = distance from pin row centerline to tube end
$D_o(D_i)$ = outside (inside)tube diameter
$D_{oj}(D_{ij})$ = outside (inside) tube diameter in attachment area
$D_{op}(D_{ip})$ = outside (inside) pin diameter
l = distance from pin row centerline to back edge of shims
L_j = total length of reinforced attachment area ($L_s + L_t$)
L_r = length of reinforcing ring
L_s = longitudinal length of metallic shim layer ($l + a$)
L_t = wall thickness transition zone
N_c = number of filament layers in tube wall that do not extend into the attachment area
N_p = number of pins along the tube circumference
N_s = number of metallic shim layers
t_a = thickness of the adhesive layer joining the metallic shim to the composite material
t_c = thickness of composite layers that do not extend between shims
t_f = thickness of composite layers between shims
t_r = maximum thickness of the transition length circumferential reinforcing rings
t_s = thickness of metallic shim layers
W = circumferential distance between pin centerlines
ω = density of the composite material
ω_a = density of the adhesive material
ω_f = density of the filler material
ω_p = density of the pin material
ω_s = density of the metallic shim material

I. Introduction

It has been determined that structural tubes fabricated of composite materials would be lighter than tubes made from more conventional materials such as steel, aluminum, or titanium alloys. However, even though structural members can be made lighter with composite materials than with the more common metal alloys, the weight of reinforcing composite tube ends and joining them to end fittings will impose penalties. As a result, the significant weight-saving potential of composite materials may tend to be offset somewhat by the weight penalties imposed by joining the tubes to end fittings. The design of efficient, lightweight joints between composite tubes and end fittings is, therefore, a necessary element in the development of composite structural components and requires formulation of design criteria and analysis techniques.

The development of joints for composite material structural members has been studied extensively by a number of investigators. Most of the previous efforts have been confined to either bonded or mechanical joints. However, both of these joint types possess inherent limitations.

This paper describes a shim-joint concept that considerably reduces these limitations and improves the efficiency of the joints. The basic geometry of the shim joint is presented in Fig. 1. The shim layers are of uniform thickness and constant length in the longitudinal direction. The composite tube end is separated into several layers and bonded to the shim layers by an adhesive. A single circumferential row of conventional shear pins is used to transfer loads from the composite tube, through the shim layers, to the mating part.

Most of the information presented thereafter refers to fiberglass composite tubes subjected to tensile load. However, this shall not be interpreted as the limitation of the shim joint concept.

The composite material used to establish design data consisted of AF-994 glass filament and Shell Chemical Company's 58-68R resin system. The shim material was AM-355 steel (ultimate tensile strength 260 ksi).

II. Analysis of Attachment Area

Mechanical fasteners in shim-reinforced composite materials produce much the same failure mode as in metals. The following analysis considers those potential failure modes resulting from axial tension loads on the joint. Net area tensile failure, pin hole bearing failure, hoop tension failure, shear bearing tearout failure, and pin shear failure can all be produced by variation of design parameters. Failure can also occur due to excessive shear in the bond joint between the shim and the composite material, or by delamina-

Presented as Paper 68-341 at the AIAA/ASME 9th Structures, Structural Dynamics and Materials Conference, Palm Springs, Calif., April 1–3, 1968; submitted March 28, 1968; revision received June 28, 1968. Work supported in part by U.S. Air Force under Contract F33(615)-67-C-1263.

* Analytical Specialist, Energy Controls Division. Member AIAA.
† Senior Engineer, Energy Controls Division.
‡ Supervisor, Filament Composites. Energy Controls Division.

tion of the fibrous layers in the tube wall thickness transition length.

Net Area Tension

Joint failure may occur in tension along the pin row centerline if the net tension area becomes sufficiently small. The ultimate strength of the net tension area depends on the ductility of the metallic shim material when a low elastic modulus composite is used. The composite material in the net tension area can support high stress if the shim can be strained sufficiently. For this reason, the combined steel and composite areas were utilized in calculating the net tension area stress.

$$A_t = (W - D_{op})[(D_o - D_i)/2 - 0.006N_c + N_s t_s] \quad (1)$$

where $W = \pi D_{oj}/N_p$. The ultimate tension load is given by

$$P_{\text{ult}} = N_p K_{tu} A_t F_{tu} \quad (2)$$

where K_{tu} is the ultimate tensile efficiency factor and F_{tu} is the ultimate tensile strength of the metal.

The allowable tensile stress is a function of the D_{op}/W ratio as in lug strength study. Flat-plate tests were conducted to determine tensile allowables and results are presented in Sec. III of this paper.

Pin Hole Bearing

Test results have indicated that bearing failure of shim-reinforced composites normally occurs as a result of shim buckling. Buckling strength is a function of individual shim thickness t_s and the unsupported metal span length D_{op}. The bearing allowables are presented in Sec. III of this paper as a function of the ratio D_{op}/t_s. The allowable pin bearing area and the ultimate tension load are

$$A_{br} = N_s t_s D_{op} \quad (3)$$

$$P_{\text{ult}} = N_p K_{br} A_{br} F_{tu} \quad (4)$$

where K_{br} is the bearing efficiency factor.

Since the failure mode is actually one of stability, the degree of restraint due to clamping must also be considered in establishing allowables for this failure mode. A joint that is tightly clamped by a threaded nut on the pin will produce much higher bearing stresses than an identical joint that is not clamped or restrained. Clamping of the flat-plate tests was adjusted to duplicate that expected in the composite tube attachment.

Hoop Tension

Hoop tension failure can occur when the pin row is placed too close to the tube end. For unidirectional composite plies, the tensile strength of the glass epoxy system is quite low in the transverse directions; therefore, the composite material was not considered to be effective in transmitting hoop stress during the establishment of allowables. Further testing would be required to establish allowables for attachments which incorporate plies oriented at an angle to the member axis. The allowable is defined in terms of the shim material ultimate tensile strength and is a function of the a/D_{op} ratio. The hoop tension area is given by the following expression:

Fig. 2 Effective bond area.

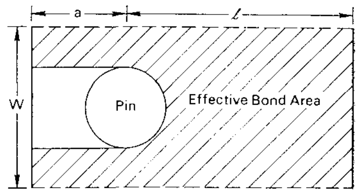

$$A_{ht} = N_s t_s[a - (D_{op}/2)] \quad (5)$$

The ultimate load for the joint is

$$P_{\text{ult}} = N_p K_{ht} A_{ht} F_{tu} \quad (6)$$

where K_{ht} is the hoop tension efficiency factor, further explained in Sec. III.

Shear Bearing

Past experience with lug design would indicate that shear bearing failure could also occur if the pin row is placed too close to the end. There were no clearly defined occurrences of shear bearing failure during the flat-plate test series of this study. It has been suggested that the tubular members may be more susceptible to shear bearing failures since the tubular geometry possesses more lateral constraints than the flat plate specimens. Only tubular test data can ascertain this fact.

Bond

To design a bonded shim joint for ultimate loading, it was necessary to use average shear strength allowables from flat-plate tests. The shim area that was considered to be effective in bond is shown in Fig. 2 to be a function of both a and l. An effective bond length l_e was defined by dividing the shaded bond area by the width W.

$$l_e = \{W(l + a) - N_p[aD_{op} + (\pi/8)D_{op}^2]\}/W \quad (7)$$

The ultimate load for a shim joint is given by

$$P_{\text{ult}} = 2N_s A_s F_s \quad (8)$$

where $A_s = l_e W$, and F_s is the allowable shear stress, defined in terms of the effective bond length l_e.

Wall Thickness Transition Zone

From a weight standpoint, it is desirable to make the transition length as short as possible (Fig. 3). As the transition length becomes shorter, however, the radial force component, which tends to separate the fibrous layers (delaminate) at the base of the transition length, becomes greater. These radial forces create tensile strain concentrations at the initial separation point of adjacent layers which must not exceed the ultimate tensile strain for the resin in the composite. The tensile strain at the separation point can be controlled by designing circ wrap reinforcement rings at both the inside and outside diameters to restrict radial move-

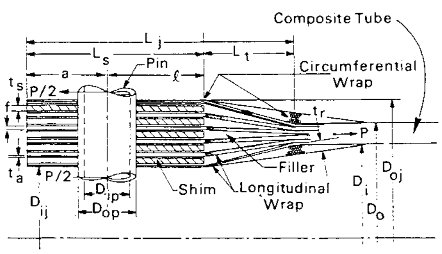

Fig. 1 Tubular shim-joint design variables.

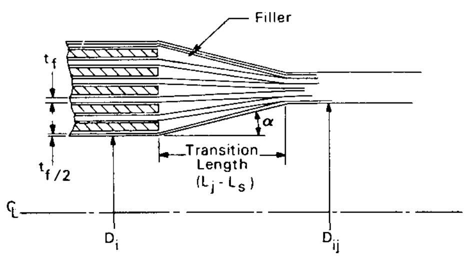

Fig. 3 Transition zone.

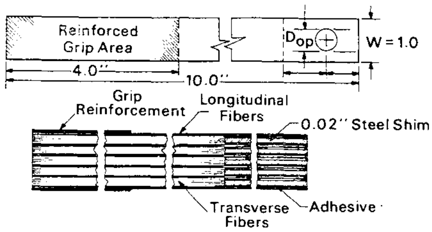

Fig. 4 Typical flat-plate specimen.

ment. The transition zone was analyzed by using a finite-element model of beams and springs. The thickness of the required reinforcing ring is

$$t_r = D_o{}^2[P_i - (P_i)_{\text{ult}}]/4E_f y_a \tag{9}$$

where P_i is the radial force on the exterior layer, $(P_i)_{\text{ult}}$ is the allowable radial force on the exterior layer, E_f is the filament modulus, and y_a the allowable radial displacement of the exterior layer. Both $(P_i)_{\text{ult}}$ and y_a values may be established through analytical-experimental studies (see Ref. 1, pp. 88, 89).

Pin Shear

The pins are loaded in double shear and the design requires simply that the cross-sectional area be large enough to insure that the shear stress does not exceed the ultimate shear strength of the material. If hollow pins are used, the ratio D_{ip}/D_{op} must be low enough to insure that the pins will not crush or buckle. The ultimate load for the pinned joint as governed by pin shear is given by

$$P_{\text{ult}} = 2N_p A_p F_{su} \tag{10}$$

where A_p is the pin area and F_{su} the ultimate shearing strength of the pin material.

III. Flat-Plate Tests

The flat-plate test specimen (Fig. 4) was developed to enable inexpensive determination of ultimate strength design allowables for the various failure modes in a shim joint. The presence of free edges on the sides of the flat-plate configuration prevents exact simulation of the tubular joint, but it is felt to be adequate for most failure modes.

The flat-plate specimen used in this study is best described by Fig. 4. Five 0.02-in. steel shim layers were used in each of the flat-plate specimens, but the other materials were included in varying quantities to produce failure modes which were of interest. The composite material was composed of 65% glass, by volume, and 35% resin. The W dimension was fixed at 1.0 in. Also, tests conducted during this study have included only longitudinal fibers between the shims. Further testing will be required to determine design allowables for shim joints in laminates having fibers oriented at an angle to the loading direction.

The specimens were loaded by a pin through the shim joint and by a friction grip on the opposite end. The shim pack was clamped lightly during the test to simulate the clamping action expected from a metal fitting mating with the reinforced tube end. The specimens were loaded to rupture to obtain ultimate strength design allowables.

Net Area Tension

The net area tension data is shown in Fig. 5. The calculated stress values were divided by the ultimate tensile strength of the shim material to form the net tension efficiency factor K_{tu}. A mean allowable curve is shown superimposed on the test data. The mean allowable is defined in terms of D_{op}/W by the expression

$$K_{tu} = 79.33/(143.75 - 100\ D_{op}/W) \tag{11}$$

which was used in the net tension area failure envelope in the design. Data points denoted as "lower-bound" values arise from tests in which failure occurred either in a different mode, or in a combination of modes that included the one of interest.

Pin Bearing

Figure 6 shows the flat-plate pin bearing strength data plotted vs the D_{op}/t_s ratio. The bearing ultimate stress values have been divided by the ultimate tensile strength of the shim material to form the pin bearing efficiency factor K_{br}. The curve was derived empirically and is defined by

$$K_{br} = 3.0 - [123.8/(107 - D_{op}/t_s)] \tag{12}$$

Equation (12) was used as the pin bearing failure envelope in the optimum design procedure.

Pin bearing failure is of special interest because it is more ductile than other failure modes. When structural members are fabricated from brittle materials such as fiberglass, it may be desirable to design the assembly such that initial failure occurs in the attachment by pin bearing to avoid catastrophic failure of the assembly.

Hoop Tension

The hoop tension test results are plotted in Fig. 7 as a function of the a/D_{op} ratio. Again a mean allowable curve has been derived to fit the test data. The mean allowable curve is obtained by

$$K_{ht} = 3.173/(a/D_{op} + 0.65) \tag{13}$$

which was used as the hoop tension failure envelope in the design procedure.

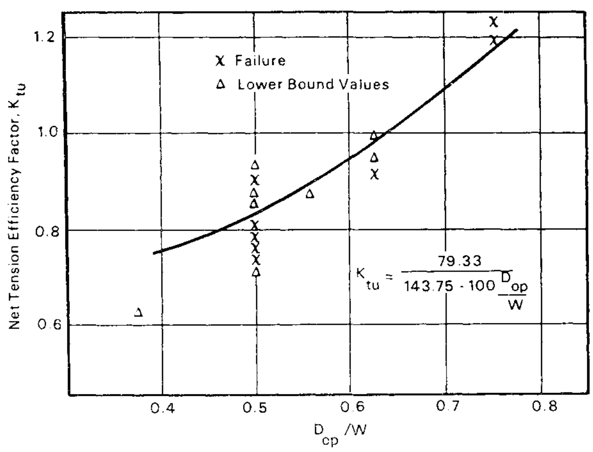

Fig. 5 Net tension test results vs D_{op}/W.

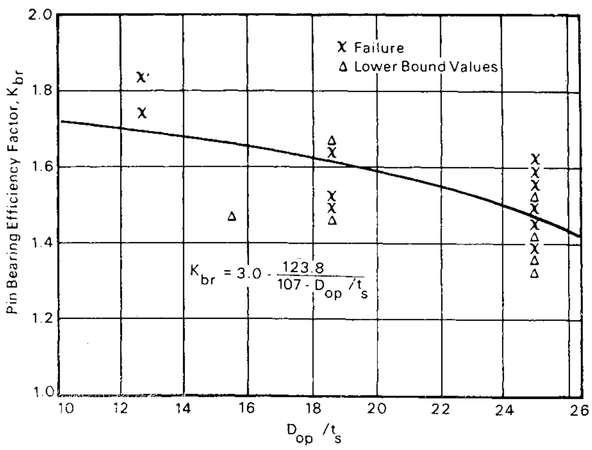

Fig. 6 Pin bearing test results vs D_{op}/t_s.

Bond

The effective length of bond for flat plates, l_e, was defined in terms of both l and a by

$$l_e = (l + a) - aD_{op} - (\pi/8)D_{op}^2 \tag{14}$$

Figure 8 shows the test data plotted vs the effective length. The solid line curve represents the bond strength of the AF-111 (3M Corporation) adhesive tape, and the dashed line curve shows the bond strength for the BR-1009-49 tack primer (American Cyanimid Corporation). An algebraic equation was derived to fit the AF-111 shear strength. The curve is defined by

$$f_s = 5130/(l_e + 1.95) \tag{15}$$

where f_s is the average adhesive shear stress.

The AF-111 adhesive film produces thicker adhesive layer than the BR-1009-49 tack primer. It can be shown that thicker adhesive layer does reduce the shear stress concentration factor (see Ref. 1, pp. 10–12, 75–87).

Transition Zone

Two flat-plate specimens were fabricated without the excess transverse fiberglass layer to study the delamination failure mode in the thickness transition zone. The specimens did fail by delamination as expected, and the data were used to establish allowable stress level in the circumferential, reinforcing ring, design procedure.

IV. Optimum Design

A feasible design is one that behaves satisfactorily under the specified conditions. In general, it is possible to find more than one feasible shim joint design for a given composite tube. If one of the design features is taken as the design objective, it is possible to find a feasible design that is most favorable as judged by the design objective. In the present study, weight was chosen as the design objective.

Design Constraints

A shim joint is considered feasible if it satisfies the following design constraints.

1) Net section tension:

$$[(\pi/2)(D_{oj} + D_{ij}) - N_pD_{op}][\tfrac{1}{2}(D_{oj} - D_{ij}) - N_ct_c + N_st_s] \times K_{tu}F_{tu} \geq P_{\text{ult}} \tag{16}$$

2) Bearing:

$$N_pD_{op}N_st_sK_{br}F_{tu} \geq P_{\text{ult}} \tag{17}$$

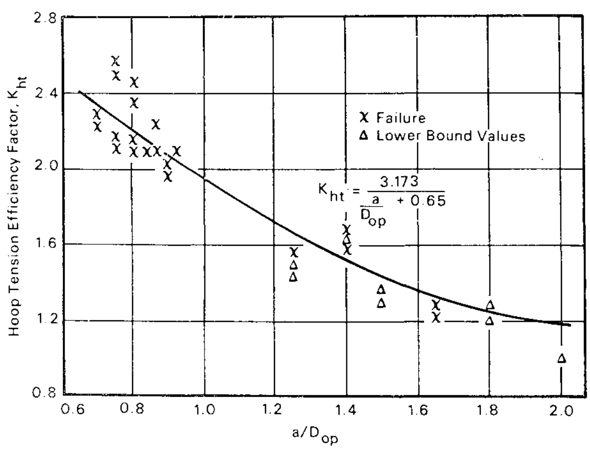

Fig. 7 Hoop tension test results vs a/D_{op}.

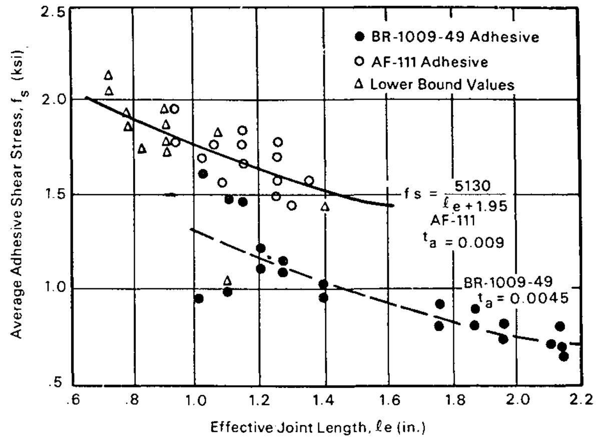

Fig. 8 Average adhesive shear strength vs effective joint length.

3) Hoop tension:

$$N_p(a - \tfrac{1}{2}D_{op})N_st_sK_{ht}F_{tu} \geq P_{\text{ult}} \tag{18}$$

4) Bond:

$$\pi N_s(D_{oj} + D_{ij})l_eF_s \geq P_{\text{ult}} \tag{19}$$

5) Circ reinforcing ring:

$$t_r \geq D_o^2[P_i - (P_i)_{\text{ult}}]/4E_{fg}y_a \tag{20}$$

6) Pin:

$$(\pi/2)N_pD_{op}^2[1 - (D_{ip}/D_{op})^2]F_{su} \geq P_{\text{ult}} \tag{21}$$

Objective Function

To write the objective function, the weight of each joint component is expressed in terms of the design variables.

1) Fiberglass composite:

$$W_{fg} = \left[\frac{\pi}{4}(D_o^2 - D_i^2)L_j - \frac{\pi}{4}D_{op}^2N_p \times \left(\frac{D_o - D_i}{2} - N_ct_c\right) - N_ct_c\pi\left(\frac{D_o + D_i}{2}\right)L_j\right]\omega \tag{22}$$

2) Shim:

$$W_s = N_st_s\{\pi[(D_{oj} + D_{ij})/2]L_s - (\pi/4)D_{op}^2N_p\}\,\omega_s \tag{23}$$

3) Circ wrap ring:

$$W_r = [2\pi(D_o + D_i)t_r^2\tan(\alpha/2)]\omega \tag{24}$$

4) Filler:

$$W_f = (\pi/4)(D_{oj} + D_{ij})N_sL_j(t_s + 2t_a)\omega_f \tag{25}$$

5) Pin:

$$W_p = \frac{\pi}{4}D_{op}^2\left[1 - \left(\frac{D_{op}}{D_{ip}}\right)^2\right]N_p \times \left[\left(\frac{D_o + D_i}{2} - N_ct_c\right) + N_s(t_s + 2t_a) + l_p\right]\omega_p \tag{26}$$

where l_p is the pin length required outside shim pack to connect the mating fixture.

As a structural member, the total length of the composite tube is fixed. An increase in the joint length naturally causes a decrease in the uniform section portion of the composite tube. Consequently, the increase of weight due to longer joint length is partially compensated by a shorter basic tube section. Since the joint length is a design parameter, the total joint weight does not reflect the additional weight superimposed to the tube.

Table 1 Results of pin number variation study

No. of pins	D_{op}, in.	l, in.	a, in.	L_t, in.	t_s, in.	t_r, in.	Objective function, lb	Total joint weight, lb
8	0.549	0.685	0.686	0.461	0.021	0.014	0.429	0.518
9	0.518	0.680	0.681	0.447	0.019	0.009	0.389	0.477
10	0.491	0.702	0.667	0.424	0.017	0.012	0.369	0.457
11	0.468	0.722	0.661	0.409	0.016	0.010	0.349	0.436
12	0.448	0.740	0.663	0.414	0.017	0.015	0.373	0.461
13	0.431	0.753	0.664	0.422	0.019	0.023	0.414	0.502

For this reason the shim-joint objective function is defined as

$$W_o = W_{fg} + W_s + W_r + W_f + W_p - (\pi/4)(D_o^2 - D_i^2)L_j\omega_{fg} \quad (27)$$

which is the weight added to the structural member by the attachment.

Optimum Design Procedure

Now the design problem may be stated as to find the minimum of Eq. (27) subjected to the condition of Eqs. (16–21). There are a number of directly applicable mathematical methods for the solution of this type problem. The method selected in this study was the steepest descent. The net attachment weight was taken as the objective function and the conditions Eqs. (16–21) were treated as constraints. Then the objective function was minimized under the constraints.

The method used is a descent routine. Starting with an initial solution, steps are taken towards new points at which the value of the objective function is improved. The iteration process continues until a minimum is reached (see Ref. 1, p. 95).

The procedure described previously has been programmed in Fortran IV to form a basic optimization routine. The routine has been used successfully for numerous design problems. When applied to the design of shim joints, the input consists of 1) number of design parameter and number of constraints, 2) limit of interative cycles, 3) initial step length, 4) tolerance range for each constraint, 5) applied load, 6) tube geometry, 7) mechanical properties of materials, 8) design constraints, 9) initial design parameters, and 10) optional information.

If allowable stress is expressed as a function of design parameters, it is convenient to incorporate allowable stress expressions in the program. The program output consists of 1) design parameters, 2) information concerning any violation of constraints, 3) direction of movement, 4) weight of each shim-joint component, and 5) value of the objective function.

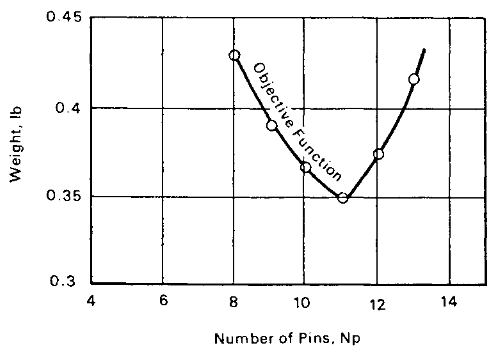

Fig. 9 Increase in weight of structural member due to joint vs number of pins used in joint.

The program was executed on an IBM 360/44 computer. Artificial constraints may be added to improve convergence. For example, the minimum practical values of a, t_s, and t_r may be treated as artificial constraints. For six design variables and eleven constraints (including artificial constraints for convenience) the average running time was 5–6 min. It was observed that usually after 25 iterations the variation of objective function was in the order of $\frac{1}{1000}$ lb. It was also observed that different sets of reasonable initial conditions all lead to practically identical objective function and design parameters. For all practical purposes the objective function obtained in 25 iterations may be taken as the minimum and the corresponding design parameters the optimum design.

Example

The optimization procedure was used to design the tubular joint for the final structural test of this program. The design allowable expressions obtained from the flat-plate data were used in the constraint equations (16–21). The design was performed with the following parameters fixed:

$$D_o = 3.0 \text{ in.} \qquad D_i = 2.928 \text{ in.}$$

$$D_{oj} = 3.095 \text{ in.} \qquad D_{ij} = 2.833 \text{ in.} \qquad D_{op}/D_{ip} = 0.8$$

$$F_{tu} = 260 \text{ ksi} \qquad F_{su} = 110 \text{ ksi}$$

$$t_a = 0.009 \text{ in.} \qquad t_c = 0.006 \text{ in.} \qquad \omega = 0.074 \text{ lb/in.}^3$$

$$\omega_s = 0.283 \text{ lb/in.}^3 \qquad \omega_f = 0.040 \text{ lb/in.}^3$$

$$N_s = 5.0 \qquad N_c = 2.0 \qquad P_{\text{ult}} = 150\ k$$

With the exception of N_p (number of pins), the remaining design parameters were allowed to vary in the optimization routine.

The routine does not handle discrete variables and it was impractical to treat N_p as a continuous variable. To determine the optimum number of pins, the number of N_p was varied in consecutive runs having otherwise identical input. The resulting joint designs are shown in Table 1. The table includes both 1) the weight added to the basic tube by the reinforcement and pins (objective function) and 2) the total weight of the joint section. The pins were considered to be hollow and made from 180 ksi ultimate tensile strength steel.

The objective function is plotted as a function of N_p in Fig. 9. As the plot indicates, the 11-pin configuration is clearly the optimum one for the specified problem.

Efficiency of the Shim-Joint Concept

A comparison can be made by studying a composite tube having shim joints with tubes of other materials designed to meet the same loading requirement. In Fig. 10 the weights of constant strength tubes have been plotted vs tube length. The metal tubes are assumed to have identical strength in tension and compression. Two curves are shown to reflect the different tensile and compressive strengths of 5,0°:1,90° fiberglass. Thin wall buckling and column buckling are not considered. The fiberglass-tube weights include 0.7 lb to reflect the weight added to both ends of the tube by the minimum weight 11-pin attachment of the previous section.

Examination of Fig. 10 reveals that for design governed by tensile strength, fiberglass tubes are more efficient than aluminum for tube length of 5.0 in. or larger and lighter than steel or titanium for tube lengths exceeding 7.5 in. If compressive strength governs the tube design, fiberglass is more efficient than aluminum for lengths greater than 6.5 in. and lighter than steel- or titanium-tube lengths exceeding 12.0 in.

V. Materials and Fabrication

Materials

The filament composite materials employed in this study consisted of AF-994 glass filaments and Shell Chemical Company's 58-68R resin system. The metal shim was made of AM-355 steel coil, 8 in. wide, 0.02 in. thick, and of continuous length. The shim cleaning procedure employed was originally developed and reported in Ref. 3.

The bond between the corrosion resistant steel shims and the filament composite material was provided by a structural adhesive. Two types of adhesives were evaluated. The first was BR-1009-49 tac, primer as supplied by the American Cyanimid Corporation, and the second was AF-111 structural adhesive fiber furnished by the 3M Corporation. BR-1009-49 tack primer was utilized during the early phase of the program. A primer coating of uniform thickness of approximately 0.005 in. was obtained and was oven cured for 60 min at 315°F. AF-111 structural film was utilized during the later phase of the program. The adhesive film was applied to the steel shim and stored at 40°F until ready for use.

Holes were drilled through the fiber-resin-shim-composite to permit insertion of shear pins. Carbide-tipped or full carbide drills were used. Holes larger than 0.250-in. diam can be drilled in successive steps of approximately 0.375-in.-diam increase per step.

Flat-Plate Specimens

The flat-plate filament composite specimens utilized in this program were specially wound on a winding machine. The test specimens were wound over 12-in. by 2-in. aluminum mandrels.

Guide blocks were provided on one end of the mandrels to facilitate locating the metal shims as they were wound into the ends of the specimens. Two specimens were wound simultaneously by utilizing both sides of the mandrel. The wrapped mandrels were then cured for 4 hr at 350°F. The specimens were removed from the mandrel by cutting the glass composite along the edges with a high-speed cutting

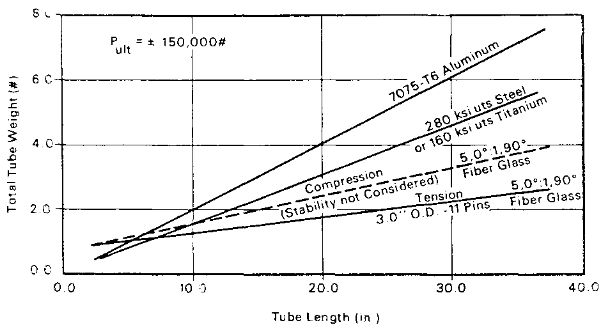

Fig. 10 Weight comparison of constant strength tubes vs tube length. Fiberglass-tube weights include steel-end reinforcement and steel pins.

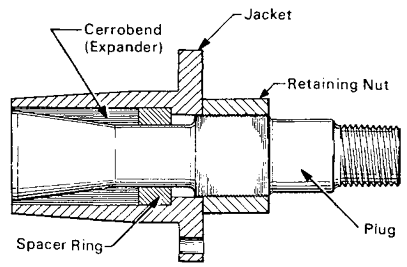

Fig. 11 Tension fixture assembly.

disk. The sides and ends were trimmed with a hand saw and flat-plate disk sander.

Tubes

Open end cylinders were fabricated two at a time by winding a double length cylinder and then cutting it into two cylinders. The cylinders were wound over mandrels machined from salt block, which was later removed by dissolving in hot water. Thin corrosion resistant steel shims, in the form of narrow circumferential bands, were wound into the cylinders on each side of the planned cut which would separate the two cylinders. Subsequent to removal of the salt mandrel, a circumferential row of holes was drilled through the wall of each cylinder in the shim area for later insertion of shear pins.

VI. Structural Test

Test Fixtures

Ultimate strength testing of the final tubular joint design required the fabrication of two separate test fixtures. One fixture is a clevis-type which mates with the reinforced attachment area of the tube to form the pin joint. The fixture was fabricated in two pieces to avoid the expensive machining which would be required by a monolithic assembly. The two pieces were held tightly together by a nut during drilling of the pin holes. The nut was used to insure that equal loads would be applied to the pins on the inside and outside diameter of the tube.

The second test fixture (see Ref. 1, pp. 97–100) held the opposite end of the tabular specimen which was reinforced only by four additional layers of filament material. The fixture employed a friction gripping technique. A schematic of the fixture is shown in Fig. 11.

Tension Test of Tubular Joint

A 3.0-in.-o.d. tube was fabricated with steel-reinforced end to test the shim-joint concept in a full-scale structural member. The test specimen was designed to fail in the attachment area since the program is oriented to refinement of shim-joint design technology. The basic tube was fabricated with a 5,0°:1,90° wrap pattern to a wall thickness of 0.072 in. The ultimate tensile load for the tube was found to be 150 kips (see Ref. 2, pp. 2–19). The attachment area was also designed to transfer 150 kips. The specimen was loaded in an Olsen Machine to an ultimate tension load of 135.5 kips. Fracture occurred in the outer fiberglass layer at the edge of the outside shim. It is felt that both the test fixtures and the shim joint did perform well.

Compression Test of Tubular Joint

The tension clevis fixture and the jacket of the friction grip fixture was used to conduct the compression test. A cerrobend plug was cast to reinforce the inside diameter of the nonreinforced tube end. The test specimen was identical to the tension specimen. The ultimate compressive load for the tube was found to be about 51.0 kips. The attachment area suffered no discernible damage.

VII. Conclusions

The following conclusions may be made: 1) design parameters can be optimized conveniently by the structural synthesis approach in determining the minimum weight configuration, and 2) the shim-joint concept can be successfully applied to composite members without prohibitive attachment weight penalties.

References

[1] Cole, B. W., Wong, J. P., and Courtney, A. L., "Development of the Shim Joint Concept for Structural Members," Tech. Rept. AFFDL-TR-67-116, Aug. 1967, Air Force Flight Dynamics Lab., Wright-Patterson Air Force Base, Ohio.

[2] "Exploratory Application of Filament Wound Reinforced Plastic for Aircraft Landing Gear," Tech. Rept. AFML-TR-66-309, Dec. 1966, The Bendix Corp., Products Aerospace Div.

[3] "Large Segmented Fiber Glass Reinforced Plastic Rocket Motor Cases," Rept. ASD-IR-8-150, Vol. I-VIII, Thiokol Chemical Corp., Wasatch Div.

[4] Goland, M. and Reissner, E., "The Joint Stresses in Cemented Joints," *Journal of Applied Mechanics*, Vol. 11, March 1944, pp. A17–A27.

[5] Melcon, M. A. and Hoblit, F. M., "Analysis of Lugs and Shear Pins," *Product Engineering*, May 1950, p. 113, and June 1953, p. 160.

[6] "Mechanics of Adhesive Bonded Lap-Type Joints: Survey and Review," Rept. ML-TDR-64-298, 1964, Forest Product Lab., U.S. Dept. of Agriculture, Madison, Wis.

[7] "Manufacturing Methods for Plastic Airframe Structures by Filament Winding," Tech. Rept. IR-9-371(1), Feb. 1967, Air Force Materials Lab., Wright-Patterson Air Force Base, Ohio.

[8] Ridha, R. A. and Wright, R. N., "Minimum Cost Design of Frames," *Journal of Structural Division, Proceedings of the American Society of Civil Engineers*, Vol. 93, ST4, Aug. 1967, Paper 5394.

JAN.-FEB. 1969 J. AIRCRAFT VOL. 6, NO. 1

Damping of High-Frequency Brake Vibrations in Aircraft Landing Gear

A. K. Abu-Akeel*
The Bendix Corporation, South Bend, Ind.

This paper outlines the nature of high-frequency brake-excited vibrations and shows how a tuned damper can effectively suppress the excitation. The problem, defined as a self-excited, two-mass system, is analyzed and a closed-form solution is obtained. An energy balance approach is utilized to treat the possible nonlinear functions present in the system. It is shown that the two resulting modes are stable within a defined range of frequency ratio and secondary system damping. This range is affected by the mass ratio and the intensity of excitation, i.e., negative damping. Stability charts are plotted to help select the optimum size, tuning, and damping conditions of a brake-tuned damper effective under actual service conditions. Experimental results are shown to confirm the theoretical analysis.

Nomenclature

C_1,C_2 = equivalent viscous damping constants of the primary and secondary systems respectively, lb sec/in.
E = energy, lb in.; subscripts i, d, and v refer to input, damped, and viscous damping energy, respectively
f_1,f_2 = primary system and secondary system (damper) positive damping functions, respectively
I_1,I_2 = total polar moment of inertia of the primary and secondary systems, respectively in. lb sec^2
K_1,K_2 = equivalent stiffness of the primary and secondary system springs, respectively, in. lb/rad
M = margin of stability; subscripts v and h for viscous and hydrodynamic damping, respectively
n_i = damping parameters of the two modes of motion, $i = 1,2$
p_i = frequency parameters of the two modes of motion, $i = 1,2$
r_i = frequency ratio, $r_i = p_i/\omega_2$, $i = 1,2$
T = torque applied to the brake, in. lb
x = frequency ratio ω_2/ω_1, a wear parameter
x_{min},x_{max} = limiting values of x, beyond which either or both modes are unstable
θ_{ij} = amplitude of system $j,(j = 1,2)$ in mode i, $i = 1,2$
θ_1,θ_2 = angular deflection of fixed parts of the brake (primary system) and of the secondary system, respectively, rad
η_i = damping parameter $= n_i/\omega_2$, $i = 1,2$
μ = I_2/I_1, mass ratio
ω_1,ω_2 = natural frequency of primary system, $(K_1/I_1)^{1/2}$ and of secondary system, (K_2/I_2),$^{1/2}$ respectively, rad/sec
ζ_1 = primary system negative damping factor $= C_1/2I_1\omega_1$
ζ_2 = secondary system positive damping factor $= C_2/2I_2\omega_2$

Presented as Paper 68-312 at the AIAA/ASME 9th Structures, Structural Dynamics, and Materials Conference, Palm Springs, Calif., April 1–3, 1968; submitted March 25, 1968; revision received July 1, 1968.

* Analytical Specialist, Energy Controls Division.

I. Introduction

Vibrations induced by brakes in landing gears have become a sizeable problem for brake manufacturers since harder cerametallic linings were introduced. The excellent wear characteristics of those linings are associated with increased braking roughness, i.e., excessive vibrations.

The three modes of vibrations usually observed during brake application, are described as follows: 1) chatter mode, involves back-and-forth oscillations (fore and aft) of the